Death-associated Protein 3 (Dap-3) Is Overexpressed in Invasive Glioblastoma Cells *in Vivo* and in Glioma Cell Lines with Induced Motility Phenotype *in Vitro*[1]

Luigi Mariani, Christian Beaudry, Wendy S. McDonough, Dominique B. Hoelzinger, Elzbieta Kaczmarek, Francisco Ponce, Stephen W. Coons, Alf Giese, Rolf W. Seiler, and Michael E. Berens[2]

Neuro-Oncology Laboratory [L. M., C. B., W. S. M., D. B. H., E. K., F. P., M. E. B.] and Department of Neuropathology [S. W. C.], Barrow Neurological Institute, Phoenix, Arizona 85013; Neurochirurgische Klinik, UKE, 20246 Hamburg, Germany [A. G.]; and University Hospital, Inselspital, 3010 Bern, Switzerland [R. W. S.]

ABSTRACT

Purpose: **To discover the genetic determinants of glioma invasion *in vivo*, we compared the mRNA expression profiles of glioblastoma cells residing at the tumor core *versus* those at the invasive rim of a human tumor resection.**

Experimental Design: **From a single glioblastoma specimen, 20,000 individual cells from each region (core and invasive rim) were collected by laser capture microdissection and analyzed by mRNA differential display. Differential expression of gene candidates was confirmed by laser capture microdissection and quantitative reverse transcription-PCR in additional glioblastoma multiforme specimens, and the role in migration was further evaluated in glioma cell lines *in vitro*.**

Results: **Reproducible overexpression the death-associated Protein 3 (Dap-3) mRNA (NM 004632, GenBank; also reported as human ionizing resistance conferring protein mRNA, HSU18321, GenBank) by invasive cells was identified. Although the full-length Dap-3 protein has been described as proapoptotic, the NH_2-terminal fragment can act in a dominant negative way resulting in protection from programmed cell death. In glioma cell lines T98G and G112 with an induced motility phenotype, Dap-3 was up-regulated at the mRNA and protein level as assessed by quantitative reverse transcription-PCR, cDNA microarray, and Western blot analysis. These cells showed an increased resistance to undergo camptothecin-induced apoptosis, which was overcome by effective Dap-3-antisense treatment. Antisense treatment also decreased the migration ability of T98G cells.**

Conclusions: **Dap-3 is up-regulated in invasive glioblastoma multiforme cells *in vivo* and in glioma cells with an induced motility phenotype *in vitro*. When migration is activated, Dap-3 is up-regulated and cells become resistant to apoptosis. These findings suggest that Dap-3 confers apoptosis-resistance when migration behavior is engaged.**

INTRODUCTION

GBM[3] almost invariably recurs locally despite surgical resection, radiation therapy, and chemotherapy (1). The ability of gliomas in general and GBMs in particular to invade the surrounding tissue diffusely and eventually regrow the tumor bulk is unique among cancer types (2–5). Although many data are available on cell motility from *in vitro* studies, the determinants of local and metastatic invasion *in vivo* are just beginning to emerge (6, 7). Genes that are critical for tumorigenesis are not only involved in cell-cycle regulation but also in migration/invasion and programmed cell death (7–14). The discovery of a specific genetic profile responsible for the invasive behavior of GBM cells *in vivo* is therefore likely to lead to new therapeutic targets.

We used a gene discovery approach implementing LCM and differential display of cDNAs to compare the gene expression profile of cells in the core and at the invading edge of frozen human GBM specimens (15). Dap-3 was identified as being overexpressed in invasive GBM cells *in vivo* and in highly motile glioma cells *in vitro*. Dap-3 has been described mainly as a positive mediator of IFN-γ-, TNF-α-, and Fas-induced apoptosis (16–18); however, Dap-3 can also confer protection from Fas-, ionizing radiation-, and streptonigrin-induced cell death (18, 19). We found that glioma cells with an induced motility phenotype overexpressing Dap-3 were more resistant to apoptosis than the parental cells.

MATERIALS AND METHODS

LCM. Cryopreserved GBM specimens from five patients were cut in serial 6–8 μm sections and mounted on uncoated

Received 1/18/01; revised 5/31/01; accepted 5/31/01.
The costs of publication of this article were defrayed in part by the payment of page charges. This article must therefore be hereby marked *advertisement* in accordance with 18 U.S.C. Section 1734 solely to indicate this fact.
[1] Supported by the Pediatric Brain Tumor Foundation of the United States. L. M. is funded by a grant from the Swiss National Research Foundation. A portion of this work represents the doctoral dissertation of Elzbieta Kaczmarek, University of Hamburg.
[2] To whom requests for reprints should be addressed, at Neuro-Oncology Laboratory, Barrow Neurological Institute, NRC 4th Floor, 350 West Thomas Road, Phoenix, AZ 85013. Phone: (602) 406-6664; Fax: (602) 406-7172; E-mail: mberens@chw.edu.

[3] The abbreviations used are: GBM, glioblastoma multiforme; LCM, laser capture microdissection; Dap-3, death-associated protein 3; TNF, tumor necrosis factor; ECM, extracellular matrix; FBS, fetal bovine serum; QRT-PCR, quantitative reverse transcription-PCR; ODN, oligodeoxynucleotide; cds, coding sequence; LSC, laser scanning cytometry; IRRC, ionizing radiation resistance-conferring.

slides treated with diethyl pyrocarbonate. The tumor core and adjacent invasive rim were identified on a coverslipped section stained with H&E. One specimen was selected for collection of 20,000 individual cells for mRNA isolation and differential display analysis; the other specimens were used for quantitative, differential RT-PCR analysis. Cryostat sections intended for LCM were transferred from −80°C storage, and immediately immersed in 75% ethanol at room temperature for 30 s. Slides were rinsed in H_2O, stained with filtered Meyer's hematoxylin for 30 s, rinsed in H_2O, stained with blueing reagent for 20–30 s, washed in 70% and 95% ethanol for 1 min each, stained with eosin Y for 20–30 s, and dehydrated in 95% ethanol (2 × 1 min), 100% ethanol (stored over a molecular sieve; 3 × 1min), and xylene (3 × 10 min). Slides were air-dried under a laminar flow for 10–30 min and immediately processed for LCM. Diethyl pyrocarbonate-treated, autoclaved, distilled water was used to prepare every solution.

LCM was performed with a PixCell II Microscope (Arcturus Engineering, Mountain View, CA) using a 7.5 μm laser beam at 50–100 mW. GBM cells in the tumor core were readily identified and captured. Tumor cells immediately adjacent to necrotic or cortical areas, cells with a small regular nucleus, endothelial cells, and blood cells were avoided. Neoplastic astrocytes in the invasive rim ~1 cm from the edge of the tumor core were identified according to the criteria of nuclear atypia (coarse chromatin, nuclear pleomorphism, multinucleation) and, when possible, according to their nuclear and/or cytoplasmic similarity with the GBM cells in the core.

Differential Display of mRNA. Approximately 20,000 individual cells from the core and the invasive rim of fresh-frozen sections of a GBM were harvested by LCM. RNA was isolated from these samples according to manufacturer's directions (Stratagene, La Jolla, CA). One hundred ng of total RNA from each population was added to duplicate reverse transcriptase reactions, each containing the oligodeoxythymidylate primer (sequence: 5′-TTTTTTTTTTTA-3′), called H-T11A, anchored to the beginning of the poly(A) tail. PCR was used to amplify random primed segments of cDNA according to the manufacturer's directions (Hunter RNAimage, Nashville, TN). Briefly, each reverse transcriptase mix was aliquotted; combined with one of eight different assorted primers (AP1–8), and tagged with ^{33}P[dATP]. A display of the cDNAs was generated in the form of bands on a 6% polyacrylamide/urea gel. Reproducible bands (determined by parallel processing mRNA extractions from the two cell populations) that were differentially expressed in either of the cell populations were excised from the gel. The cDNA was reamplified using the appropriate matching assorted primer (H-AP1) and H-T_{11}A primer, then cloned using a TA Cloning Kit (Invitrogen, San Diego, CA). Bacterial colonies were plated on agar containing 50 μg/ml ampicillin and 40 μl of 40 mg/ml 5-bromo-4-chloro-3-indolyl-β-D-galactopyranoside. Colonies carrying the plasmids with inserts (white in color) were harvested, expanded, verified using *Eco*RI restriction digestion, and sequenced using a CEQ2000 automated sequencer (Beckman). From these candidates two bands of interest were elected for in-depth analysis.

QRT-PCR. From four additional GBM biopsy specimens, approximately 1000 cells were captured from the tumor core and the invasive rim by LCM and further processed for RNA isolation (Stratagene). Isolates were processed into cDNA using reverse transcriptase according to the manufacturer's protocol (Ambion). cDNA for histone H3.3 was used for quantitative normalization of harvested material in the matched rim-core analyses.

Real-time quantitative PCR was performed using the LightCycler (Roche), which exploits the ability of SYBR-green to fluoresce after hybridization with double-stranded DNA. SYBR-green fluorescence was detected in real time after each cycle of amplification (20, 21). The primer sequences for Dap-3 were as follows: forward, 5′-GGAATTAGCACGTGTTCACA-3′; and reverse 5′-CATAAAGCAGATGTCCACTG-3′ (amplicon size, 389 bp). PCR conditions for Dap-3 were as follows: denaturation at 95°C for 30 s and then 40 cycles of 95°C for 0 s.; 67°C for 7 s.; 72°C for 18 s.; and then the melting curve analysis was done. Primers for histone H3.3 were as follows: forward, 5′-CCACTGAACTTCTGATTCGC-3′; reverse, 5′-GCGTGC-TAGCTGGATGTCTT-3′ (amplicon size, 215 bp). PCR conditions for histone H3.3 were as follows: 40 cycles of 95°C for 0 s.; 64°C for 6 s.; 72°C for 20 s.; and then the melting curve analysis was done (22).

Internal standards of templates for quantitative analysis of the gene of interest were prepared by cloning *Dap-3* and *Histone H3.3* sequences compatible with the specific primers into the pCR 2.1 TOPO TA vector (Invitrogen). After expansion in *Escherichia coli*, plasmids were extracted and linearized, and the concentration of DNA was determined by absorption at 260 nm. Serial dilutions of the 50 μg/ml stock template solutions were used as standards with a known number of copies of Dap-3 and Histone H3.3 cDNA. PCR was performed on two μl of DNA (template standard or clinical sample) in a final volume of 20 μl. Analysis of the melting curves (standards *versus* sample and negative control) ensured specificity of the amplification for the expected product. Additionally, agarose gel electrophoresis of the PCR products was followed by staining with ethidium bromide to confirm the specificity of the amplification based on the molecular weight of the amplicons.

Quantification was performed on the initial exponential phase of amplification above baseline according to the LightCycler software (20, 21). The calculated cDNA copy number in each sample was derived from an extrapolated crossing point of a mathematically derived line extending from the exponential phase of amplification in a plot of fluorescence intensity (SYBR-green) *versus* cycle number. Diluted known standards of templates provided quantitative standard curves for each gene of interest against which the unknown clinical specimens were compared. Histone H3.3 was used as a housekeeping gene to normalize the initial content of total cDNA in the paired samples from the tumor core and from the invasive rim. The rim-core ratio, $r = X/Y$, was calculated, where X is the Dap-3 copy number in the rim and Y is the Dap-3 copy number in the core, both normalized to equivalent amounts of histone H3.3.

Induction of Migration of Glioma Cell Lines on Cell-derived ECM and Laminin. To create a coating of cell-derived ECM proteins, culture flasks were seeded with SF767 glioma cells. The cells were grown in MEM supplemented with 10% FBS to postconfluence. They were removed by treatment with Triton X-100 0.5% for 30 min at room temperature, and then by NH_4OH 0.25 M for 3–5 min at room temperature, and

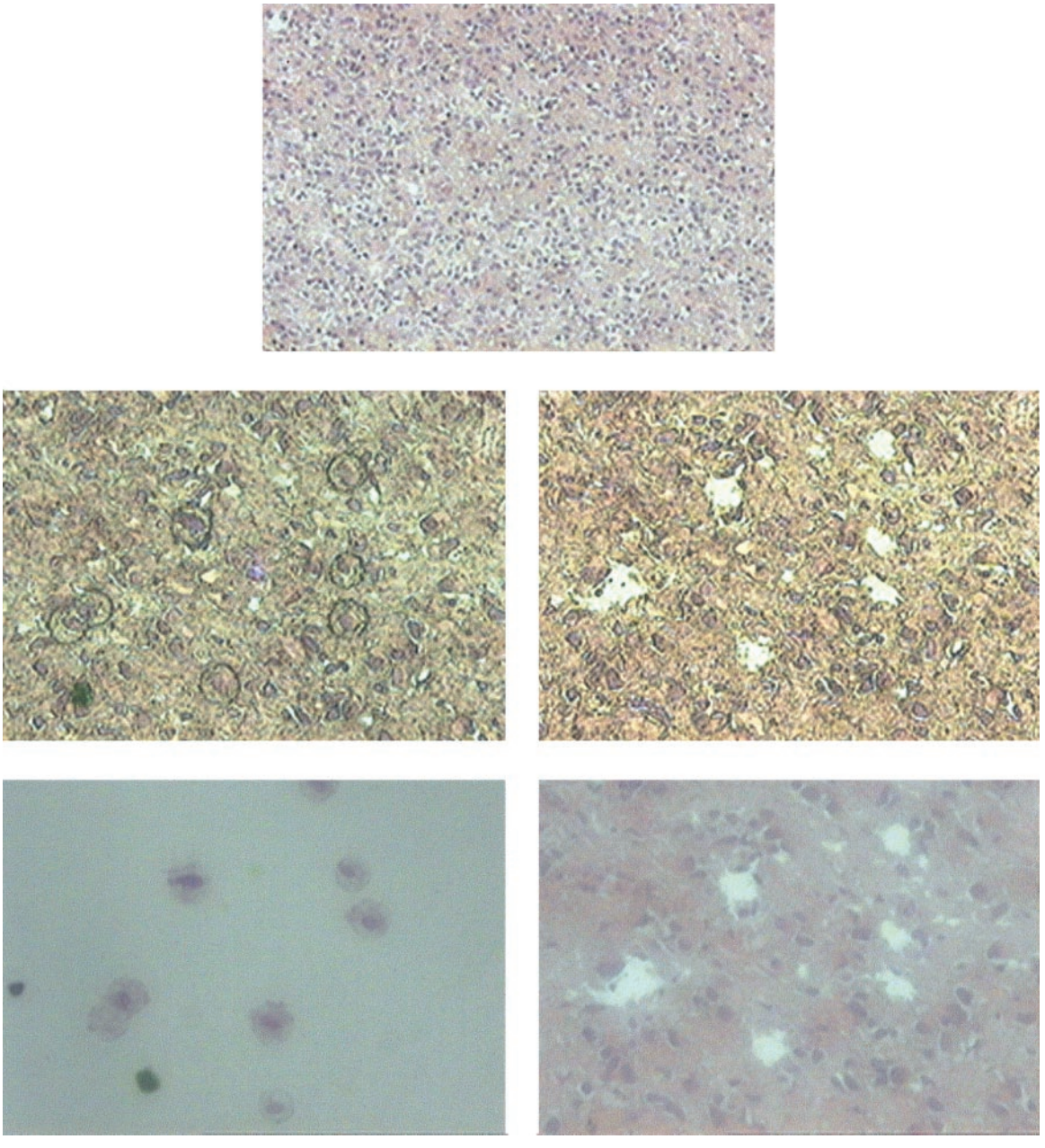

Fig. 1 LCM technique at the invasive edge. *Top* microphotograph shows the invasive edge of a human GBM specimen at ×10 after H&E-staining and coverslipping. *Middle*, view of the same area at ×20 through the LCM microscope without visualizer. *Left*, cells have been selected as invasive tumor cells on the basis of their morphology: mainly large nuclear size and atypical nuclear shape. The polymer cap on these cells has been hit by a laser beam of 7.5 μm in diameter and 50 mV power. After the polymer cap is removed, the *open* areas demonstrate the absence of microdissected single cells (*middle panel, right*). The same region (*right*) and the captured cells (*left*) are shown through a visualizer in the *bottom row*.

thoroughly rinsed with PBS (23, 24). The flasks covered with cell-derived ECM proteins were stored at 4°C until used. Alternatively, culture flasks were coated with laminin (10 μg/ml) during 1 h at 37°C and then thoroughly rinsed with 1× PBS.

T98G and G112 glioma cells were seeded either on untreated flasks or on ECM- or laminin-coated flasks to induce a migratory phenotype. The cells were grown to 30–50% confluence, then trypsinized, counted, aliquotted, and additionally processed for QRT-PCR as described above or for protein analysis.

cDNA Microarray Analysis. G112 glioma cells were seeded on plain roller bottles culture flasks or on flasks coated with SF767-derived ECM and grown until 40–60% confluency. Approximately 40 million cells/sample were harvested by trypsinization for isolation of total RNA (Qiagen RNeasy Maxi Kit). Total RNA was further purified with TRIzol (Life Tech-

nologies, Inc.); RNA concentrations were measured by spectrophotometry and normalized accordingly. Reverse transcription was performed using the SuperScript II reverse transcriptase (Life Technologies, Inc.), incorporating Cy3-dUTP in cDNA from 80 μg total RNA from cells grown on plastic and Cy5-dUTP in cDNA from 150 μg total RNA from cells grown on ECM. In a second reverse transcription reaction for a separate hybridization, the cDNA was labeled with the reciprocal fluorochrome. cDNAs probes were purified and concentrated with Microcon-30 columns (Amicon) mixed with a hybridization cocktail containing 15 μg of poly(dA), 6 μg of yeast tRNA, 15 μg of CoT 10 DNA, 2× Denhardt's solution, 2.7× SSC-0.2% SDS, denatured, and hybridized at 65°C on a 6.712-k cDNA microarray chip (NIH) for16 h. Slides were washed in 0.1% SDS with 0.5× SSC-0.01% SDS with 0.5× SSC and 0.06× SSC for 2 min each at room temperature and scanned (6).

Immunohistochemistry Studies. Fresh frozen tissue blocks were sectioned (6 μm thick) onto slides, then fixed in freshly prepared paraformaldehyde (2%) for 30 min, and rinsed with PBS. Sections were incubated at room temperature with 0.1% Triton X-100 for 10 min to permeabilize the membranes. To quench endogenous peroxidase activity, slides were incubated for 30 min in 0.3% hydrogen peroxide in water. To block nonspecific binding, slides were incubated in 10% goat serum in PBS at room temperature for 30 min. Slides were washed in PBS, then incubated with mouse antihuman Dap-3 IgG1,1:400 (Transduction Laboratories, Kentucky), or no primary antibody, for the negative control, for 1 h at room temperature. Slides were washed in PBS for 5 min and the secondary antibody, goat antimouse IgG-biotin, was added at a 1:500 dilution in PBS. Slides were incubated for 1 h at room temperature. After rinsing in PBS for 5 min, slides were incubated with VECTASTAIN Elite ABC reagent (Vector Laboratories) for 30 min at room temperature. The slides were rinsed with PBS for 5 min and developed in diaminobenzidine peroxidase substrate solution (Sigma Chemical Co.) for 2 min. The reaction was stopped with tap water. The slides were counterstained with Mayer's hematoxylin and coverslipped.

Antisense Studies. Phosporothioate ODNs were designed from the cds of the Dap-3 mRNA as follows: antisense ODN, 5′-GCTGTGATCTTGGCTTAGAGGTA-3′ (complementary to bp no. 1262 until no. 1284 of the cds); mismatch ODN, 5′-CTGTGGCTATGTCGTGATGAGAT-3′. T98G and G112 glioma cells were grown to 40–60% confluence in 10-cm tissue culture dishes in MEM supplemented with 10% FBS. The calcium-phosphate precipitation method was used for transfection following a typical protocol (25). Cells were treated with either a calcium phosphate precipitate (1× HBSS, 0.125 mM CaCl2, and H_2O) alone or with the precipitate containing 7–18 μg of the phosphorothioate oligonucleotides for 12 h in MEM + 10% FBS in a standard incubator. The cells were then trypsinized, counted, and seeded for the migration assay. An aliquot of collected cells was used for QRT-PCR and for protein analysis.

Migration Assay. The microliter scale migration assay has been detailed previously (26, 27) and recently has been used to verify *in vitro* the invasive phenotype observed *in vivo* (6). Briefly, 10-well slides were coated with BSA 1% or laminin 10 μg/ml at 37°C for 1 h. Approximately 2500 cells/well were seeded into a cell sedimentation manifold (CSM, Inc., Phoenix, AZ) to establish a confluent monolayer circle within a 1-mm diameter. Cells were allowed to migrate during 24 h in MEM supplemented with 10% FBS at 37°C. The migration rate was calculated as the radius increase of the entire cell population. Experiments were performed as five replicates. At the end of the migration, the slides were fixed in 2% paraformaldehyde or 70% ethanol and processed for Dap-3 immunostaining and quantitative analysis of immunofluorescence by laser scanner cytometry.

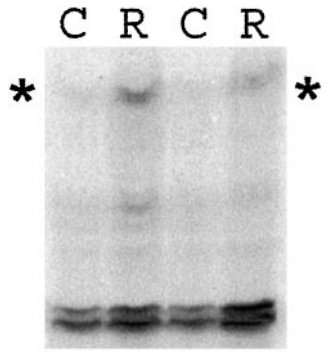

Fig. 2 Differential display analysis of mRNA. mRNA-differential display analysis of LCM-collected cells from the tumor core (*C*) and invasive rim (*R*) of a human GBM specimen. Isolated RNA from the LCM-collected material was equally divided and then processed in duplicate to determine reproducibility of the differential display. The cDNA band (flanked by ∗) was excised and amplified using H-11TA and AP1 primer sets. The cDNA sequence of this band seemed to be overexpressed by the invasive tumor cell population compared with the cell population of the tumor core. The sequence of this cDNA was 97% homologous with *Dap-3* mRNA.

Viability Assays after Treatment with ODNs. The AlamarBlue assay (28) was used to test for the potential toxic effect of ODNs on glioma cell lines. Alamar blue incorporates an oxidation-reduction indicator that fluoresces and changes color in response to chemical reduction of growth medium resulting from cell growth. Briefly, cells were grown to 60% confluency before treatment with either 2.5 μM antisense or 2.5 μM mismatched ODNs overnight. After 6 h of treatment, 4000 cells of each population were seeded in quadruplicate wells of three 96-well flat-bottomed plates in 200 μl of culture medium supplemented with 10% FBS. The plates were incubated for 4, 20, and 32 h, respectively. Alamar blue was added in a volume of 20 μl (10% of total volume) to the cells at the various time points and incubated for 2 h. The plates were read on a fluorescence plate reader (excitation, 530 nm; emission, 590 nm). Averages of the absorbance values were calculated and plotted against a standard curve of untreated cells to assess increases in cell number over time.

Western Blot Analysis for the Dap-3 Protein. After multiple washes with PBS, the cells were lysed in 100 μl/million cells of protein lysis buffer containing protease inhibitors.

A protein assay was performed to normalize the protein concentration among samples (BCA Protein Assay Reagent; Pierce). An identical volume of electrophoresis buffer 2× [24.8 mM Tris base, 192 mM Glycine, 0.1% w/v SDS, bromphenol blue in 1 liter dH_2O (pH 8.3)] was added to the sample, which

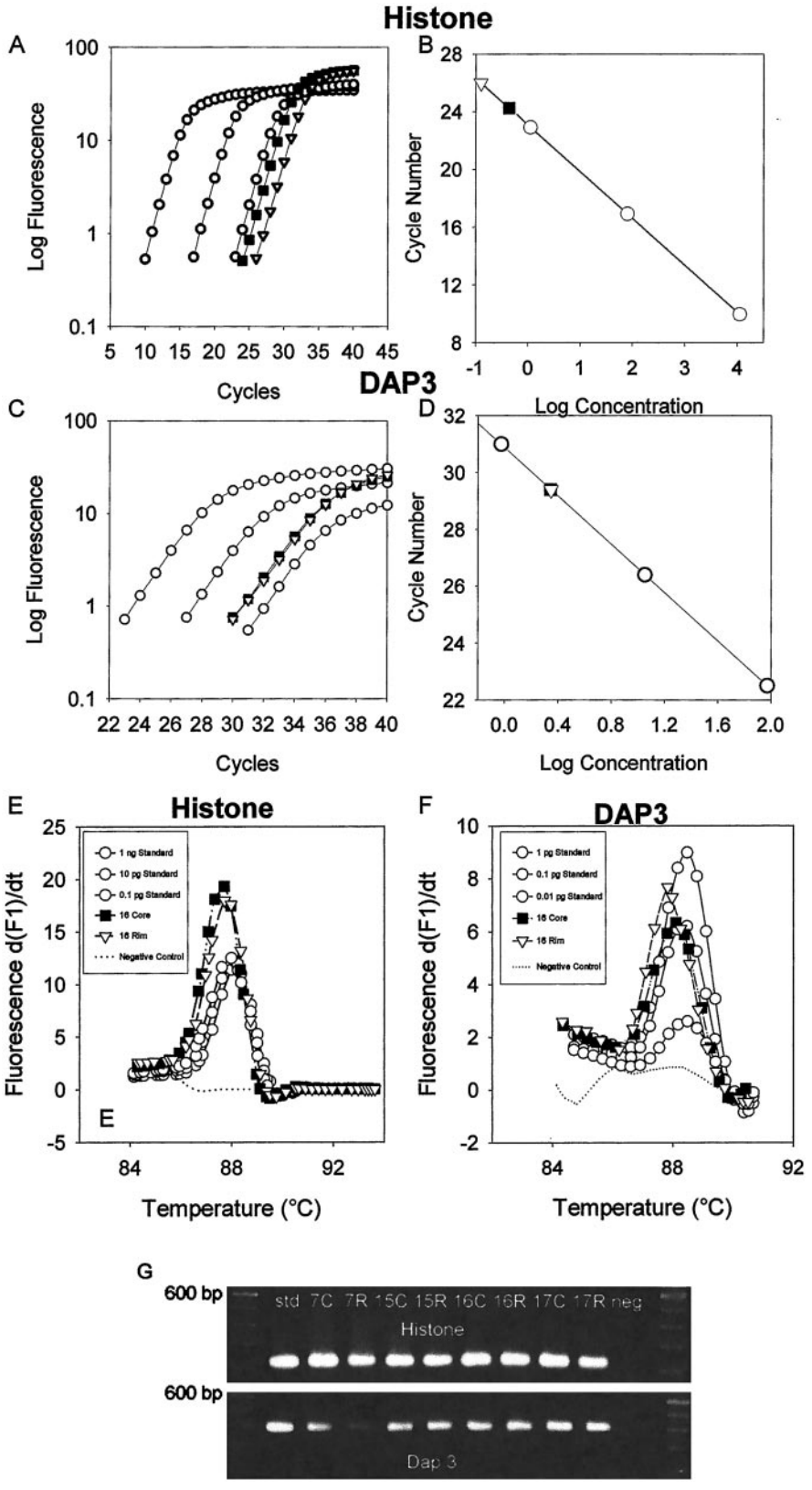

Fig. 3 QRT-PCR analysis. *A–D,* typical, exponential, PCR amplification curve is shown for five cDNA samples: three serial dilutions of the standards (*A,* histone H3.3; *C,* Dap-3) and the cDNA from the tumor core (■) and invasive rim (△) of specimen 16. Amplicon abundance (log fluorescence) increased with the number of PCR cycles. A threshold level of fluorescence is selected above background. The number of cycles necessary to produce detectable fluorescence above background during the early exponential phase was determined. The standards of known concentration were used to draw a standard curve (*B* and *D*) where the samples of core and rim were plotted to calculate the number of copies of histone H3.3 (for normalization) and Dap-3, respectively (*E–G*) Analysis of the melting curve of the PCR product (*E,* for histone H3.3; *F,* for Dap-3) suggested high amplicon specificity for the standards and the core and rim samples. Amplicon specificity was confirmed further by agarose gel electrophoresis (*G*).

was boiled for 10 min. Twenty- to 50-μl aliquots of the sample and 10 μl of the molecular weight marker were separated on a 12.5% acrylamide gel in an electrophoretic chamber at 150–200 mA current for ~1 h. The proteins were transferred to a nitrocellulose membrane (Protran) using a protein transfer buffer [24.8 mM Tris base, 192 mM glycine, and 10% vol/vol methanol in 1 liter dH_2O (pH 8.3)] in a transfer chamber at 300 mA for ~1 h. The nitrocellulose membrane was blocked in 5% nonfat dry milk in dH_2O overnight at 4°C and washed 3× 10 min with 0.05% Tween 20 in PBS. The membrane was then incubated with the anti-Dap-3 primary antibody (catalog no. D56620; mouse, IgG1; Transduction Laboratories; 1:1000 dilution), washed 3× 10 min with 0.05% Tween 20 in PBS and then incubated with a goat antimouse IgG (H+L) biotin-conjugated secondary antibody (Pierce) in ddH_2O for 1 h and washed 3× 10 min with 0.05% Tween 20 in PBS. Finally, the membrane was incubated with streptavidin-horse radish peroxidase (Amersham Life Science) for 30 min and with a mixture of the same amount of Solutions No. 1 and No. 2 of the ECL Detection reagent (Amersham Pharmacia Biotech) at the final volume of 0.125 ml/cm^2 membrane. The membrane was exposed to a photosensitive film (Kodak Scientific Imaging Films) and developed. The film was visualized with a digital camera and the intensity of the bands was quantified using GelExpert (NucleoTech) software.

LSC. LSC was used to quantify the level of Dap-3 protein at the end of the migration assay on different substrates and after treatment with Dap-3-antisense or mismatched oligonucleotides. LSC is based on the same principles as flow cytometry, but is done on a slide. After Dap-3-immunofluorescent staining of the migration assays, the slides were processed using a laser scanning cytometer (CompuCyte; Cambridge, MA). The amount of fluorescence (FITC, green) was recorded for each single cell of a migration assay. The mean peak channel fluorescence of every migration assay, reflecting the amount of Dap-3-staining, was used as a parameter for quantification. The mean peak channel fluorescence of migration assays on BSA or ECM treated with either antisense-ODNs or mismatch-ODNs was quantified.

Induction and Detection of Apoptosis in Glioma Cells. Camptothecin-induced apoptosis in the T98G cells was performed in a 96-well plate. One-half of the plate was coated with 10 μg/ml laminin and another region was left uncoated. Approximately 2×10^5 cells were seeded in every well the day before apoptosis induction. The cells were treated for 24 h with 0.125, 0.25, 0.5, and 1 μM of camptothecin. The DePsipher assay (R&D Systems) was then used to assess apoptosis in T98G cells. DePsipher is a lipophylic cation (5,5′,6,6′-tetrachloro-1,1′,3,3′-tetraethylbenzimidazolyl carbocyanine iodide) that aggregates upon membrane polarization to form an orange-red fluorescent compound. Failure of the mitochondrial transmembrane potential, called ψ, is one of the first intracellular changes in apoptosis (29). If the potential is disturbed, the dye cannot access the transmembrane space and remains or reverts to its green monomeric form. After treatment with camptothecin, cells were incubated with a DePsipher solution for 20 min. The red fluorescence representing live cells was measured at 485/590 nm using a microtiter-plate reader. A standard curve plotting a known number of live cells and the corresponding amount of red fluorescence without treatment was used to assess the number of living cells after every experiment.

Table 1 Rim/core ratio for Dap-3

Specimen no.	Rim/Core ratio RT no. 1	Rim/Core ratio RT no. 2
7	8.2	2.9
15	3.4	3.1
16	20.0	3.4
17	10.4	10.8
Mean	8.7	4.3
Range (±1 SD)	4.2–18.2	2.3–7.9
P (*t* test, two-tailed)	0.010	0.019

RESULTS

Overexpression of Dap-3 by the Invasive Tumor Cells *in Vivo*. Approximately 20,000 individual cells were harvested from both the tumor core and the invasive rim of frozen sections of one GBM specimen using LCM (see Fig. 1). The isolated RNA was reverse transcribed into cDNA in duplicate reactions. Differential display between the two cDNA populations revealed 50–60 bands of reproducible, dissimilar intensities on autoradiograms. Discrete cDNA bands differentially expressed using the primer set H-T11A and H-AP1 (clone R1.3) were consistently overexpressed in the rim cell population (Fig. 2). A sequence homology of 97% was found with the 3′-end of the cds of Dap-3 mRNA and the IRRC protein mRNA (498 of 509 bp and 433 of 444 bp, respectively).

The Dap-3 mRNA (WWW Blast at NCBI; NM 004632) has 1608 bp; the IRRC mRNA has 1648 bp (WWW Blast at NCBI; U18321). The sequences of Dap-3 and IRRC are 99% homologous (1485/1489 bp). Accordingly, we considered them as the same cDNA sequence discovered using different approaches and reported by two different authors (17, 19).

To confirm overexpression of Dap-3 in invasive cells, ~1000 cells from both the invasive rim and core of four GBM specimens from different patients were harvested by LCM. RNA was isolated from the cells and processed for QRT-PCR analysis. Real-time monitoring of increasing amplicon abundance allowed quantification of template copy number in the original samples. Quantification was achieved using standards of the targeted PCR template for the gene of interest at known copy numbers run with the samples of unknown concentration, as exemplified in Fig. 3, *A–D*. Verification of amplicon identity was done by analysis of the melting curve of the DNA (Fig. 3, *E–F*), and molecular weight determination of the product in agarose gel electrophoresis of the product (Fig. 3*G*). The samples from the tumor core and the invasive rim were normalized according to the housekeeping gene. The ratio or Dap-3 copy number rim/core varied between 3.1 and 20 (summarized in Table 1). The ratios from two separate reverse transcription reactions (RT 1 and RT 2) in the four specimens were as follows: 8.2 (RT 1) and 2.9 (RT 2) for specimen 7; 3.4 and 3.1 for specimen 15; 20 and 3.4 for specimen 16; and 10.4 and 10.8 for specimen 17. We compared all of the ratio values with the theoretical value of 1 (null hypothesis) using the unpaired Student's *t* test and obtained a *P* of 0.006. When the same test was

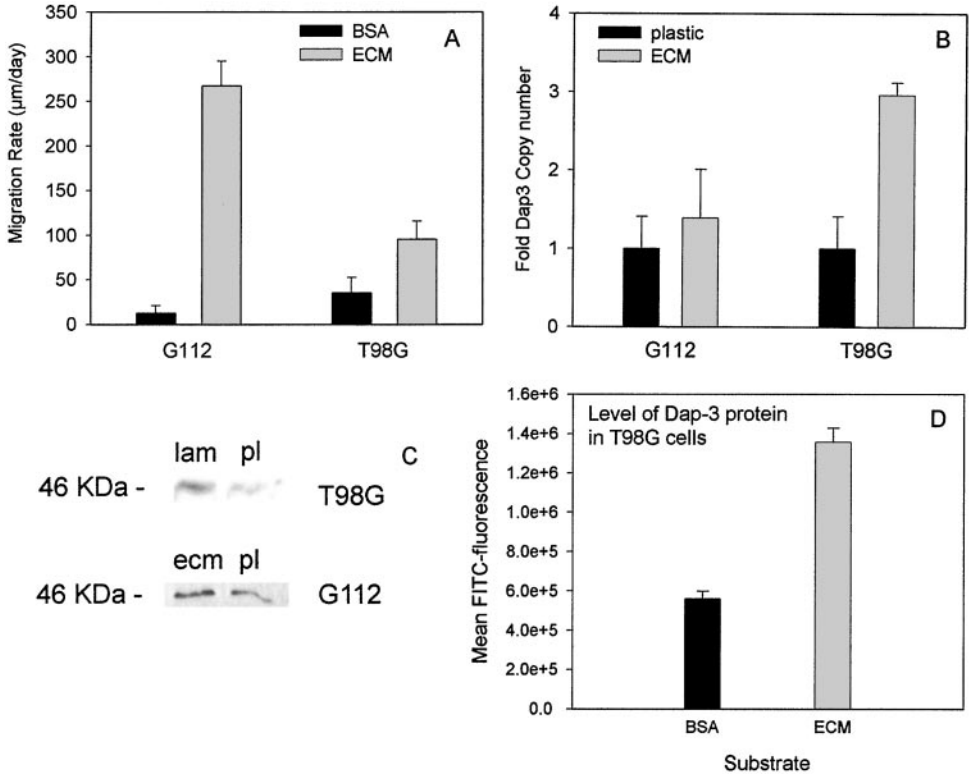

Fig. 4 Overexpression of Dap-3 in migrating cells. *A*, the migration rate of G112 and T98G cells is greater when the cells are spread on motility-inducing substrates, in this case cell-derived ECM proteins, as compared with an unspecific substrate (BSA). In this particular experiment, G112 cells were more responsive to ECM-treatment than T98G cells. Other independent experiments did not confirm this finding but always indicated a significant motility-response of both cell lines on ECM (not shown). *B*, the number of copies of Dap-3 mRNA was calculated using QRT-PCR in cells grown on plastic or on ECM. T98G cells showed a clear overexpression of Dap-3 on ECM. *C*, Western blot analysis using a monoclonal anti-Dap-3 antibody qualitatively confirmed overexpression at the protein level in both cell lines (by 2.1-fold in G112 cells and by 2.2-fold in T98G cells using analysis of band intensity) on ECM compared with plastic (*pl*). *D*, overexpression of Dap-3 at the protein level was confirmed further in T98G cells using LSC. *Bars*, 1 SD from the mean of 5 (*A*) and 3 replicate experiments (*B* and *D*).

used for each separate specimen, $P = 0.22$ for specimen 7, $P = 0.0044$ for specimen 15, $P = 0.326$ for specimen 16, and $P = 0.00043$ for specimen 17. Overall these results confirmed overexpression of the Dap-3 mRNA in the invasive GBM cells compared with cells residing in the tumor core.

Overexpression of Dap-3 in Glioma Cells on Migration-promoting Substrates. Human glioma cell lines G112 and T98G were grown either in standard culture flasks or in flasks in duplicates or triplicate. The flasks were either precoated with glioma-derived ECM or laminin or left untreated. ECM and laminin both enhance the motility behavior of these cells (30, 31; Fig. 4*A*). Total RNA was isolated from each flask to perform QRT-PCR analysis of Dap-3 expression in duplicate. The samples were normalized according to the number of copies of histone h3.3 and lamin B. The whole experiment was performed three times for every cell line, and the results were consistent. Fig. 4*B* shows the results of one of these experiments. There was a clear and statistically significant overexpression of the Dap-3 mRNA in T98G cells seeded on ECM and on laminin (~3-fold) and a marginal overexpression in G112 cells. A discrete up-regulation by 1.63-fold of Dap-3 in G112 cells on ECM was confirmed by cDNA microarray analysis (not shown). Analysis of the band intensity of a Western blot using a monoclonal antibody directed against Dap-3 qualitatively confirmed overexpression of Dap-3 at the protein level (Fig. 4*C*). Quantitative analysis of the level Dap-3 protein using laser scanner cytometry further confirmed overexpression in T98G cells on ECM (Fig. 4*D*).

The immunochemistry studies on one frozen GBM specimen (specimen 16) showed the presence of specific immunostaining for Dap-3 in the cytoplasm of tumor cells (not shown). The fluorescent immunocytochemistry of T98G cells showed mainly perinuclear staining (not shown).

Reduced Migration of Glioma Cell Lines Treated with Antisense Dap-3-ODNs. Expression of Dap-3 in glioma cells is amenable to manipulation by treatment with antisense ODNs designed against the 3′ end of the Dap-3 mRNA. Human glioma cell line T98G showed specific reduction in Dap-3 mRNA and protein levels after treatment with antisense-Dap-3 ODNs compared with treatment with mismatch ODNs (Fig. 5, *A* and *B*). The dose-dependent reduction in levels of Dap-3 protein with antisense treatment was confirmed by laser scanner cytometry (not shown). The migration rate of T98G cells treated with antisense ODNs was moderately but significantly decreased in a dose-dependent fashion (Fig. 5*C*).

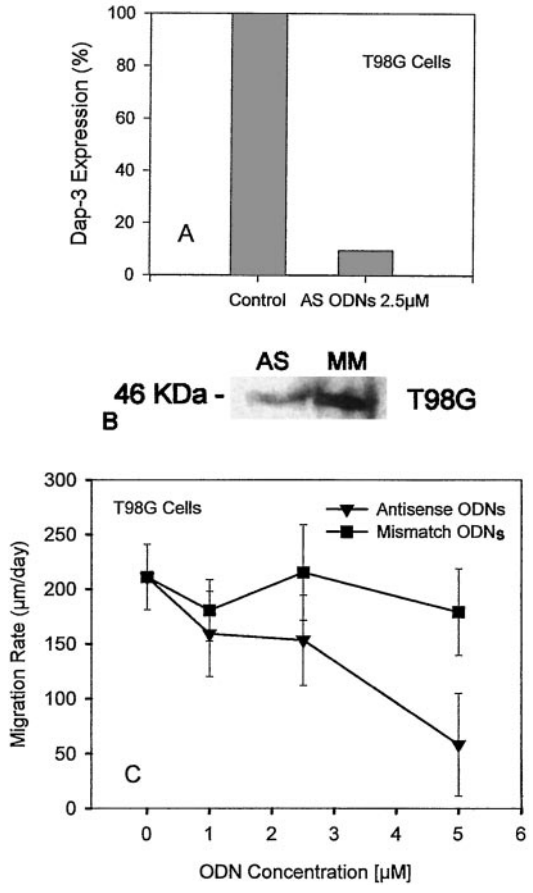

Fig. 5 Effect of antisense-Dap-3 treatment on cell migration. *A,* to demonstrate the specific effect of antisense-Dap-3 treatment on the levels of Dap-3 mRNA, QRT-PCR was performed. Antisense treatment could reduce the levels of Dap-3 mRNA down to ~7% of the level in the control (cells treated with calcium phosphate alone). The specific reduction of Dap-3 was confirmed also using a mismatched ODN as a control (data not shown). *B,* Western blot analysis using a anti-Dap-3 monoclonal antibody shows reduction of the Dap-3 protein levels in T98G cells treated with antisense ODNs compared with cells treated with mismatched ODNs (*MM*). *C,* increasing concentrations of antisense-Dap-3 ODNs reduced the migration ability of T98G cells on ECM in a dose-dependent fashion.

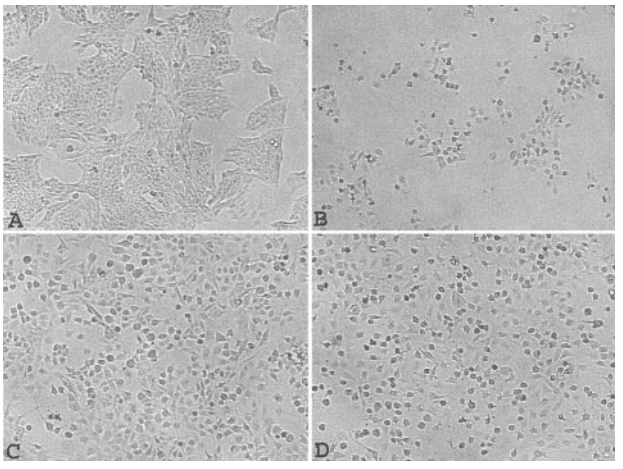

Fig. 6 Increased resistance to apoptosis of T98G cells on a motility-promoting substrate. An identical number of T98G glioma cells was seeded either on uncoated culture flasks or on culture flasks coated with laminin at 10 μg/ml concentration. The cells were grown for 3–5 days to ~70% confluence. The morphology of the cells on laminin (*C*) is strikingly different compared with the same cells on plastic (*A*). On laminin, the cytoplasmic boundaries are stretched out and the number of cytoplasmic processes (lamellipodia) is higher; as a consequence, every cell occupies more space. After treatment with camptothecin at a 1 μM concentration for 24 h, cell death was extensive on uncoated flasks (*B*) as compared with laminin-coated flasks (*D*), which were far more resistant.

Apoptosis Resistance in Migrating Cells Overexpressing Dap-3. T98G gliomas cells growing on a motility-enhancing substrate like laminin or cell-derived ECM were more resistant to apoptosis induced by camptothecin than were the cells growing on uncoated culture flasks (Fig. 6, *A–D*, and 7*A*). Exposure to camptothecin 1 μM for 22 h resulted in extensive cell detachment and death in uncoated culture flasks compared with flasks coated with laminin or ECM. Using the DePsipher assay on a microtiter plate with subsequent automated fluorescence reading allowed for the analysis of many replicates and thus for statistical significance. When T98G cells growing on plain plastic were treated with 0.5 μM camptothecin, about 70% of live cells were consistently detected after 24 h. When T98G cells were seeded on laminin 10 μg/ml and treated with 0.5 μM camptothecin, >95% of the cells remained alive after 24 h (Fig. 7*A*). This resistance to apoptosis was at least partially reversed when the cells were pretreated with Dap-3-antisense ODNs (Figs. 6 and 7*B*). This finding suggests that the survival advantage while the cells are growing on a motility-promoting substrate is at least in part related to a higher level of Dap-3.

DISCUSSION

To identify potential genetic determinants of glioma invasion *in vivo*, we implemented LCM, differential display of mRNA, and QRT-PCR. We compared the gene expression profile of GBM cells in the tumor core with those at the invasive rim. The major caveat of LCM at the invasive edge of a GBM specimen resides in the difficulty of reliably identifying tumor cells and differentiating them from normal or reactive astrocytes and other glial or neuronal cells on a frozen section stained with H&E (32, 33). To reduce the risk of harvesting normal cells, we captured cells in the immediate vicinity of the tumoral edge in the white matter. We strictly selected cells with large, dysplastic nuclei and cells similar to those in the frank tumor tissue. LCM of large cell numbers for expression profiling is very time-consuming. Interestingly, it was possible to provide a sufficient amount of useful RNA to perform gene differential display from 20,000 cells and to perform analysis by QRT-PCR from ~1,000 cells. That >99% of the cDNA sequences of the differential display were similarly expressed in the two cell populations was expected. Tumor cells at the invasive edge are hypothesized to differ from those in the tumor core because of the particular local environment to which they are exposed and because of their invasive behavior.

Dap-3 was overexpressed in invasive cells by a factor of 3–10 in five GBM specimens. Because of the potential problems

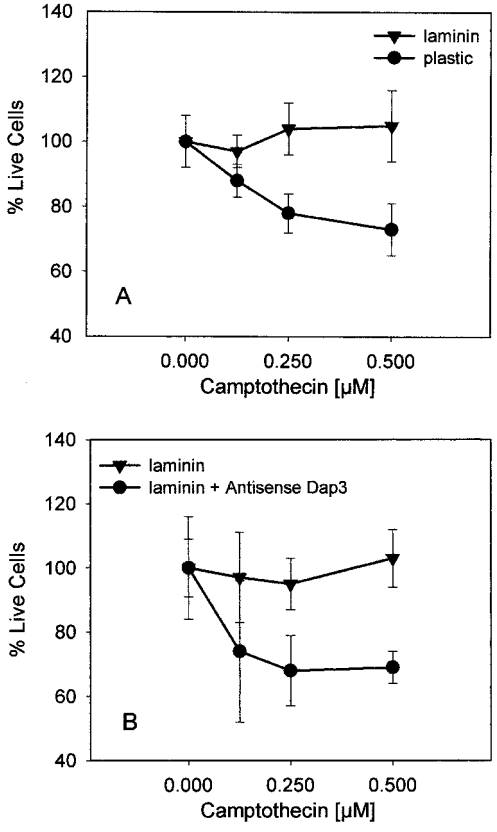

Fig. 7 Resistance to apoptosis on laminin can be overcome with Dap-3-antisense treatment. *A*, the percentage of live cells after treatment with camptothecin is significantly higher when T98G cells are exposed to laminin, which is motility-promoting. *B*, sensitivity to camptothecin-induced apoptosis of T98G cells on laminin can be restored after treatment with Dap-3-antisense ODNs. The cells were treated for about 22 h with camptothecin at a 1 μM concentration.

with LCM and because of the conceptual and technical limitations related to performing QRT-PCR on small amounts of RNA, we focused our attention on an *in vitro* strategy to further validate *Dap-3* as a potential glioma invasion gene. Exposure of glioma cells to laminin or to cell-derived ECM enhances their motility behavior, which can be tested with a migration assay. The migration rate *in vitro* strongly correlates with invasiveness *in vivo* (6, 34). overexpression of Dap-3 mRNA and protein on laminin and ECM was confirmed *in vitro*, particularly in T98G cells.

Dap-3 has been described as a proapoptotic protein downstream of the receptor/ligand complexes related to IFN-γ, TNF-α, and Fas by Kissil *et al.* (17, 18, 35, 36). They found that HeLa cells expressing antisense RNA against the *Dap-3* gene were provided with a growth advantage in a selective environment containing the cell-death inducer IFN-γ (17). They subsequently localized this gene on the chromosome 1q21 by *in situ* hybridization (36). The gene encodes a M_r 46,000 protein containing a ATP/GTP-binding domain (P-loop). The full-length protein was shown to be proapoptotic on cells exposed to TNF-α or to the agonistic Fas-antibody, whereas a P-loop mutant was less effective in inducing apoptosis, and the COOH-terminal deleted protein (230 amino acids) acted in a dominant negative fashion, protecting cells from induced apoptosis (18). More recently, Berger *et al.* (37) have shown that Dap-3 is a member of a well-conserved family of mitochondrial proteins. Hulkko *et al.* (38) showed that Dap-3 can interact with the glucocorticoid receptor, with other nuclear receptors, and with some basic helix-loop-helix/Per-Arnt-Sim proteins. Interestingly, the same cDNA encoding for Dap-3 was isolated by Henning (19) for its ability to complement functionally streptonigrin and ionizing radiation sensitivity of ataxia telangiectasia cells (AT-D) in culture. Transfection of cells with this IRRP cDNA conferred resistance to ionizing radiation- and streptonigrin-mediated apoptosis (19). Also, Kissil *et al.* (18) have demonstrated that the NH_2 terminus of Dap-3 has dominant negative effects on apoptosis. The protein has an ATP/GTP-binding (P-loop) domain and other potential binding sites (37, 38), which suggest that it might have multiple functions and/or might be implicated in different pathways. From our data, we infer that Dap-3 can sustain cell migration, that cells exposed to motility-promoting substrates become more resistant to apoptosis, and that, at least to a certain extent, the Dap-3 protein protects the cells from undergoing apoptosis. We postulate that integrin-activation increases the level of Dap-3 to sustain migration, and that this secondary activation causes a switch in function that decreases the proapoptotic activity of Dap-3. Given the overexpression of Dap-3 by invasive GBM cells *in vivo*, we can speculate that this protein can render these cells more resistant to radiation therapy and chemotherapy.

Our findings corroborate the emerging body of data linking invasiveness (7, 14) and suppressed apoptosis. Moreover, various tumor suppressor genes, *e.g., p53* (11, 39) and *PTEN* (8–10), or oncogenes, *e.g., vSrc* (12) and *Ras* (13), are linked to invasion-promoting and antiapoptotic pathway events.

ACKNOWLEDGMENTS

We are indebted to Jeffrey M. Trent (NIH, Bethesda, MD) for providing us with the microarray data and to Jim Borree from CompuCyte, Cambridge, MA, for generating the laser scanner cytometry data.

REFERENCES

1. Davis, F. G., Freels, S., Grutsch, J., Barlas, S., and Brem S. Survival rates in patients with primary malignant brain tumors stratified by patient age and tumor histological type: an analysis based on surveillance, epidemiology, and end results (SEER) data, 1973–1991. J. Neurosurg., *88:* 1–10, 1998.

2. Kelly, P. J., Daumas-Duport, C., Scheithauer, B. W., Kall, B. A., and Kispert, D. B. Stereotactic histologic correlations of computed tomography- and magnetic resonance imaging-defined abnormalities in patients with glial neoplasms. Mayo Clin. Proc., *62:* 450–459, 1987.

3. Dalrymple, S. J., Parisi, J. E., Roche, P. C., Ziesmer, S. C., Scheithauer, B. W., and Kelly, P. J. Changes in proliferating cell nuclear antigen expression in GBM multiforme cells along a stereotactic biopsy trajectory. Neurosurgery (Baltimore), *35:* 1036–1044, 1994.

4. Earnest, F., IV, Kelly, P. J., Scheithauer, B. W., Kall, B. A., Cascino, T. L., Ehman, R. L., Forbes, G. S., and Axley, P. L. Cerebral astrocytomas: histopathologic correlation of MR and CT contrast enhancement with stereotactic biopsy. Radiology, *166:* 823–827, 1988.

5. Kelly, P. J., Daumas-Duport, C., Kispert, D. B., Kall, B. A., Scheithauer, B. W., and Illig, J. J. Imaging-based stereotaxic serial biopsies in untreated intracranial glial neoplasms. J. Neurosurg., *66:* 865–874, 1987.

6. Bittner, M., Meltzer, P., Chen, Y., Jiang, Y., Seftor, E., Hendrix, M., Radmacher, M., Simon, R., Yakhini, Z., Ben Dor, A., Sampas, N., Dougherty, E., Wang, E., Marincola, F., Gooden, C., Lueders, J., Glatfelter, A., Pollock, P., Carpten, J., Gillanders, E., Leja, D., Dietrich, K., Beaudry, C., Berens, M., Alberts, D., and Sondak, V. Molecular classification of cutaneous malignant melanoma by gene expression profiling. Nature (Lond.), *406:* 536–540, 2000.

7. Clark, E. A., Golub, T. R., Lander, E. S., and Hynes, R. O. Genomic analysis of metastasis reveals an essential role for RhoC. Nature (Lond.), *406:* 532–535, 2000.

8. Maier, D., Jones, G., Li, X., Schonthal, A. H., Gratzl, O., van Meir, E. G., and Merlo, A. The PTEN lipid phosphatase domain is not required to inhibit invasion of glioma cells. Cancer Res., *59:* 5479–5482, 1999.

9. Nakamura, N., Ramaswamy, S., Vazquez, F., Signoretti, S., Loda, M., and Sellers, W. R. Forkhead transcription factors are critical effectors of cell death and cell cycle arrest downstream of PTEN. Mol. Cell. Biol., *20:* 8969–8982, 2000.

10. Tamura, M., Gu, J., Tran, H., and Yamada, K. M. *PTEN* gene and integrin signaling in cancer. J. Natl. Cancer Inst. (Bethesda), *91:* 1820–1808, 1999.

11. Bachelder, R. E., Marchetti, A., Falcioni, R., Soddu, S., and Mercurio, A. M. Activation of p53 function in carcinoma cells by the α6β4 integrin. J. Biol. Chem., *274:* 20733–20737, 1999.

12. Carragher, N. O., Fincham, V. J., Riley, D., and Frame, M. C. Cleavage of focal adhesion kinase by different proteases during Src-regulated transformation and apoptosis: distinct roles for calpain and caspases. J. Biol. Chem., *276:* 4270–4275, 2001.

13. Hernandez-Alcoceba, R., del Peso, L., and Lacal, J. C. The Ras family of GTPases in cancer cell invasion. Cell Mol. Life Sci., *57:* 65–76, 2000.

14. Niu, M., and Nachmias, V. T. Increased resistance to apoptosis in cells overexpressing thymosin β four: a role for focal adhesion kinase pp125FAK. Cell Adhes. Commun., *7:* 311–320, 2000.

15. Mariani, L., McDonough, W., Hoelzinger, D., Beaudry, C., Kaczmarek, E., Coons, S. W., Giese, A., Seiler, R., and Berens, M. Overexpression of the *P311* gene is associated with the invasive behavior of human glioblastoma cells *in vivo* and their migratory behavior *in vitro*. Cancer Res., *61:* 4190–4196, 2001.

16. Kimchi, A. DAP kinase and DAP-3: novel positive mediators of apoptosis. Ann. Rheum. Dis., *58* (Suppl.)*:* s14–s19, 1999.

17. Kissil, J. L., Deiss, L. P., Bayewitch, M., Raveh, T., Khaspekov, G., and Kimchi, A. Isolation of DAP-3, a novel mediator of interferon-γ-induced cell death. J. Biol. Chem., *270:* 27932–27936, 1995.

18. Kissil, J. L., Cohen, O., Raveh, T., and Kimchi, A. Structure-function analysis of an evolutionary conserved protein, DAP-3, which mediates TNF-α- and Fas-induced cell death. EMBO J., *18:* 353–362, 1999.

19. Henning, K. A. The molecular genetics of human diseases with defective DNA processing. Thesis (Ph.D.), Stanford University, 165 pp., 1993.

20. Roche Biochemicals LightCycler Operators Manual. *Version 3.0*, 2000.

21. Morrison, T. B., Weis, J. J., and Wittwer, C. T. Quantification of low-copy transcripts by continuous SYBR Green I monitoring during amplification. Biotechniques, *24:* 954–958, 1998.

22. Ririe, K. M., Rasmussen, R. P., and Wittwer, C. T. Product differentiation by analysis of DNA melting curves during the polymerase chain reaction. Anal. Biochem., *245:* 154–160, 1997.

23. Jones, P. A. Construction of an artificial blood vessel wall from cultured endothelial and smooth muscle cells. Proc. Natl. Acad. Sci. USA, *76:* 1882–1886, 1986.

24. Vlodavsky, I., Levi, A., Lax, I., Fuks, Z., and Schlessinger, J. Induction of cell attachment and morphological differentiation in a pheochromocytoma cell line and embryonal sensory cells by the extracellular matrix. Dev. Biol., *93:* 285–300, 1982.

25. Standard protocol for calcium phosphate-mediated transfection of adherent cells. *In:* Sambrook, J., Fritsch, E. F., and Maniatis, T. (eds.), Molecular Cloning: A Laboratory Manual/E. F., pp. 16.33–16.36. Cold Spring Harbor, NY: Cold Spring Harbor Laboratory Press, 1989.

26. Berens, M. E., Rief, M. D., Loo, M. A., and Giese, A. The role of extracellular matrix in human astrocytoma migration and proliferation studied in a microliter scale assay. Clin. Exp. Metastasis, *12:* 405–415, 1994.

27. Mariani, L., McDonough, W., Hoelzinger, D., Beaudry, C., Kaczmarek, E., Coons, S. W., Giese, A., Seiler, R., Moghaddam, M., and Berens, M. Identification and validation of *P311* as a GBM invasion gene using laser capture microdissection. Cancer Res., *61:* 4190–4196, 2001.

28. Pagé, B., Pagé, M., and Noël, C. A new fluorometric assay for cytotoxicity measurements *in vitro*. Int. J. Oncol., *3:* 473–479, 1993.

29. Yamada, H., Tada-Oikawa, S., Uchida, A., and Kawanishi, S. TRAIL causes cleavage of bid by caspase-8 and loss of mitochondrial membrane potential resulting in apoptosis in BJAB cells. Biochem. Biophys. Res. Commun., *265:* 130–133, 1999.

30. Giese, A., Rief, M. D., Loo, M. A., and Berens, M. E. Determinants of human astrocytoma migration. Cancer Res., *54:* 3897–3904, 1994.

31. Giese, A., Loo, M. A., Rief, M. D., Tran, N., and Berens, M. E. Substrates for astrocytoma invasion. Neurosurgery (Baltimore), *37:* 294–301, 1995.

32. Schiffer, D., Giordana, M. T., Mauro, A., and Migheli, A. Reactive astrocytes in the morphologic composition of peripheral areas of gliomas. Tumori, *74:* 411–420, 1988.

33. Zapata, E. J. Astrocytes in brain tumors. Differentiation or trapping? Histol. Histopathol., *9:* 325–332, 1994.

34. Chicoine, M. R., and Silbergeld, D. L. The *in vitro* motility of human gliomas increases with increasing grade of malignancy. Cancer (Phila.), *75:* 2904–2909, 1995.

35. Kissil, J. L., and Kimchi, A. Death-associated proteins: from gene identification to the analysis of their apoptotic and tumor suppressive functions. Mol. Med. Today, *4:* 268–274, 1998.

36. Kissil, J. L., and Kimchi, A. Assignment of death associated protein 3 (DAP-3) to human chromosome 1q21 by *in situ* hybridization. Cytogenet. Cell Genet., *77:* 252, 1997.

37. Berger, T., Brigl, M., Herrmann, J. M., Vielhauer, V., Luckow, B., Schlondorff, D., and Kretzler, M. The apoptosis mediator mDAP-3 is a novel member of a conserved family of mitochondrial proteins. J. Cell Sci., *113:* 3603–3612, 2000.

38. Hulkko, S. M., Wakui, H., and Zilliacus, J. The pro-apoptotic protein death-associated protein 3 (DAP-3) interacts with the glucocorticoid receptor and affects the receptor function. Biochem. J., *349:* 885–893, 2000.

39. Marchenko, N. D., Zaika, A., and Moll, U. M. Death signal-induced localization of p53 protein to mitochondria. A potential role in apoptotic signaling. J. Biol. Chem., *275:* 16202–16212, 2000.